*Transactions of the Korean Nuclear Society Spring Meeting*
*Jeju, Korea, May 29-30, 2014*

# Non-overlapping Local/Global (NLG) Iteration Scheme for 2D Transient Method of Characteristics (MOC)

Bumhee Cho and Nam Zin Cho*
*Korea Advanced Institute of Science and Technology (KAIST)*
*291 Daehak-ro, Yuseong-gu*
*Daejeon, Korea, 305-701*
*Corresponding author : nzcho@kaist.ac.kr*

## 1. Introduction

As modern computing systems become increasingly powerful, whole-core transport calculations look more promising in the near future. However, the amount of memory required for whole-core transport calculations is quite demanding [1], and computing performance still needs to be enhanced. To lessen these issues, non-overlapping local/global (NLG) iteration has been proposed [2]. The advantages of NLG iteration are that it is natural for parallel computing and competitive to the partial current-based Coarse Mesh Finite Difference (p-CMFD) [3] acceleration in terms of computing performance. Up to now, NLG iteration has been developed only for steady-state transport calculation.

In this paper, NLG iteration is extended to have the capability of transient transport calculation. As a transient transport kernel, the method of characteristics (MOC) is chosen, and applied to several test problems.

## 2. NLG Iteration Scheme

In NLG iteration, local problems are solved by transport calculation while the global problem is solved by p-CMFD. The local problems are coupled with the global problem via local interface boundary conditions.

### *2.1. Local Problem by Transient MOC*

The time-dependent transport equation through a characteristic line at a given discretized angle $j$ is given as:

$$\begin{aligned}&\frac{1}{v_g}\frac{\partial \psi_g^j(t)}{\partial t}+\sin\theta_j\frac{\partial \psi_g^j}{\partial p}+\Sigma_{t,g}\psi_g^j=\\&\quad\frac{1}{4\pi}\left[\sum_{g'=1}^{G}\Sigma_{s0,g'\to g}\phi_{g'}+(1-\beta)\frac{\chi_g}{k_{eff}}\sum_{g'=1}^{G}\nu\Sigma_{f,g'}\phi_{g'}\right.\\&\quad\left.+\chi_{d,g}\sum_{m=1}^{M}\lambda_m C_m(t)\right],\\&\frac{\partial C_m(t)}{\partial t}=-\lambda_m C_m+\frac{\beta_m}{k_{eff}}\sum_{g'=1}^{G}\nu\Sigma_{f,g'}\phi_{g'},\end{aligned}\quad(1)$$

where all notations are standard in reactor physics.

The delayed neutron precursors are integrated analytically with the assumption that the fission source is a second-order polynomial in time. In addition, a fully implicit method is applied to the time derivatives of the angular fluxes, and it is assumed that the time discretization terms of the angular fluxes are isotropic to avoid huge memory requirements [4]. With the above assumptions, the following time discretized equation is obtained:

$$\sin\theta_j\frac{\partial \psi_g^j}{\partial p}+\Sigma_{t,g}\psi_g^j=\tilde{q}_g+\sum_{g'=1}^{G}\Sigma_{s0,g'\to g}\phi_{g'}(t_{n+1}),\quad(2)$$

where $\tilde{q}_g$ includes the fission source, delayed neutron precursor source, and time discretization source.

### *2.2. Global Problem by p-CMFD*

After homogenization, condensation into $MG$, and volume integration on cell $I$ (or computational coarse mesh) for every local problem, the following equation is obtained:

$$\begin{aligned}&\sum_{u=x,y}\sum_{s=0,1}\frac{J_{G,u,s}^{+,I}(t_{n+1})-J_{G,u,s}^{-,I}(t_{n+1})}{H_u^I}+\Sigma_{r,G}^I\phi_G^I(t_{n+1})=\\&\quad\tilde{Q}_G^I+\sum_{G'=1,G'\neq G}^{MG}\Sigma_{s0,G'\to G}^I\phi_{G'}^I(t_{n+1}),\ G=1,\ldots,MG.\end{aligned}\quad(3)$$

In p-CMFD formulation, the partial currents are given as:

$$\begin{aligned}J_{G,u,s}^{+,I}&=\frac{-\tilde{D}_{G,u,s}\left(\phi_G^{I^{u,s}}-\phi_G^I\right)+2\hat{D}_{G,u,s}^{+}\phi_G^I}{2},\\J_{G,u,s}^{-,I}&=\frac{\tilde{D}_{G,u,s}\left(\phi_G^{I^{s*}}-\phi_G^I\right)+2\hat{D}_{G,u,s}^{-}\phi_G^{I^{u,s}}}{2},\end{aligned}\quad(4)$$

where

$I^{u,s}$ = the nearest coarse mesh to the coarse mesh $I$ on surface $u$, $s$.

### *2.3. Iteration Framework*

In NLG iteration scheme, the local domain size is identical to an assembly size. The local problems are solved under fixed incoming angular flux as the boundary condition. The incoming angular fluxes are

updated by the partial currents, that are in turn results of global p-CMFD, as:

$$\psi_{g,u,s}^{j,new} = \frac{J_{G,u,s}^{-,I}}{\overline{J}_{G,u,s}^{-,local}} \psi_{g,u,s}^{j,old}. \quad (5)$$

The advantage of p-CMFD is that the partial currents are the direct results of p-CMFD, while they are not available in CMFD. Therefore, if the global problem is solved by CMFD, the incoming angular fluxes must be updated under some approximations [2].

After all local problems are solved, the homogenization and condensation are performed. With homogenized parameters, global p-CMFD is solved.

The NLG iteration is continued until the fission source is converged. If the NLG iteration is converged, a new NLG iteration is performed at a new time step with initial conditions. The initial conditions of the NLG iterations of the new time step are taken from the results of the NLG iteration of previous time step in order to have good initial conditions.

## 3. Numerical Results

NLG iteration and p-CMFD acceleration have been implemented in the in-house code, SPARTA. Two test problems are solved by SPARTA and compared to the results by other codes. The results of other codes are available elsewhere [5].

### *3.1 TWIGL 2G Problem*

The first problem is the TWIGL 2G problem [6], and the geometry is shown in Fig. 1. The transient event occurs by changing the cross sections linearly (in time) of region 1. The calculation conditions for SPARTA is set to be similar to those of DeCART [7]. The steady-state results are shown in Table I.

As shown in Table I, eigenvalues are the same for NLG iteration and p-CMFD, and they agreed well with those of DeCART and VARIANT-K [8]. In addition, the computing performances are quite similar for both NLG iteration and p-CMFD acceleration.

Table I. Steady-state results : TWIGL 2G

| Code | SPARTA | | DeCART | VARIANT-K |
|---|---|---|---|---|
| Method | MOC | | MOC | Variational Nodal Method |
| Acceleration | p-CMFD acceleration | NLG iteration | CMFD | - |
| $k_{eff}$ | 0.91598 | 0.91598 | 0.91605 | 0.91609 |
| Calculation time (sec) | 241 | 246 | - | - |
| # of NLG (or outer) iterations | 14 | 15 | - | - |

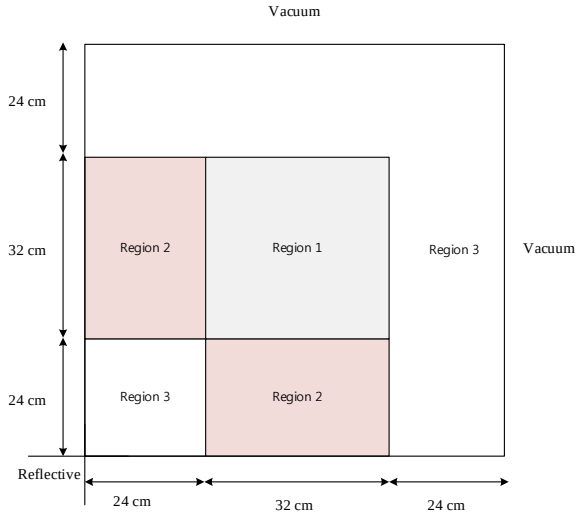


Fig. 1. Geometry : TWIGL 2G

The transient results are shown in Table II, Fig. 2, and Table III. The results of SPARTA are overlaid on the results given in [5].

In transient calculations, the computing performances are similar for both NLG iteration and p-CMFD acceleration as in the case of steady-state calculations. This is due to the good initial conditions available for NLG iteration at every time step. The power changes over time agreed well with those by other codes.

Table II. Regional power comparison : TWIGL 2G

| Time | Region | VARIANT-K | DeCART | SPARTA | |
|---|---|---|---|---|---|
| | | | | p-CMFD acceleration | NLG iteartion |
| 0 | 1 | 1.570 | 1.570 | 1.570 | 1.570 |
| | 2 | 1.994 | 1.994 | 1.994 | 1.994 |
| | 3 | 0.451 | 0.450 | 0.450 | 0.450 |
| 0.1 | 1 | 1.594 | 1.594 | 1.594 | 1.594 |
| | 2 | 1.982 | 1.982 | 1.982 | 1.982 |
| | 3 | 0.449 | 0.449 | 0.449 | 0.449 |
| 0.2 | 1 | 1.618 | 1.618 | 1.618 | 1.618 |
| | 2 | 1.969 | 1.970 | 1.970 | 1.970 |
| | 3 | 0.448 | 0.447 | 0.447 | 0.447 |
| 0.3 | 1 | 1.536 | 1.537 | 1.537 | 1.537 |
| | 2 | 2.011 | 2.012 | 2.011 | 2.011 |
| | 3 | 0.453 | 0.452 | 0.452 | 0.452 |
| 0.4 | 1 | 1.526 | 1.526 | 1.526 | 1.526 |
| | 2 | 2.017 | 2.017 | 2.017 | 2.017 |
| | 3 | 0.453 | 0.453 | 0.453 | 0.453 |
| 0.5 | 1 | 1.570 | 1.569 | 1.570 | 1.570 |
| | 2 | 1.994 | 1.995 | 1.994 | 1.994 |
| | 3 | 0.451 | 0.450 | 0.450 | 0.450 |

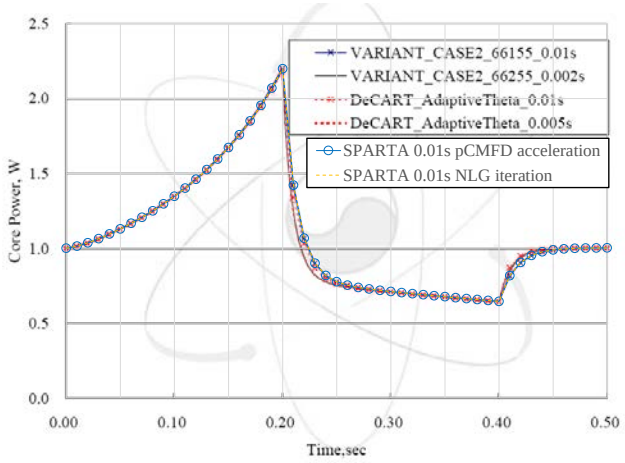


Fig. 2. Power vs time : TWIGL 2G

Table III. Computing time for transient : TWIGL 2G

| Code | SPARTA | |
|---|---|---|
| Acceleration | p-CMFD acceleration | NLG iteration |
| Calculation time (sec) | 5418 | 5614 |

### *3.2 Mini-core 2D Problem*

The second problem is the Mini-core 2D problem [9]. The geometry is shown in Fig. 3. The transient event occurs by linearly changing the cross sections of UOXR.

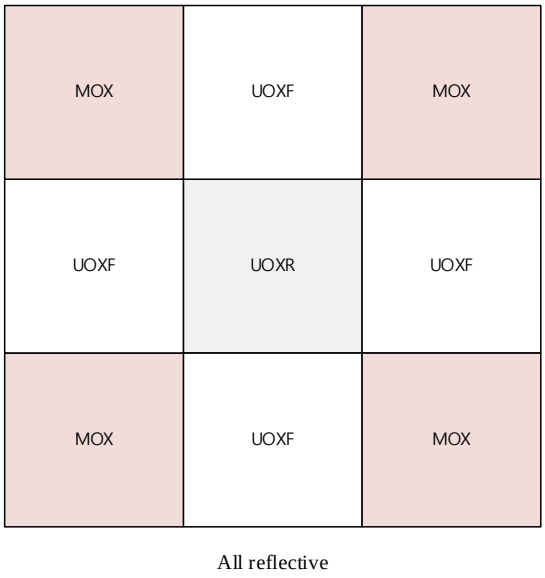


Fig. 3. Geometry : Mini-core 2D

The steady-state results are shown in Table IV. All eigenvalues agreed well. The computing performance of p-CMFD acceleration and NLG iteration are similar.

Table IV. Steady-state results : Mini-core 2D

| Code | SPARTA | | DeCART | VARIANT-K |
|---|---|---|---|---|
| | p-CMFD acceleration | NLG iteration | | |
| $k_{eff}$ | 1.05644 | 1.05644 | 1.05644 | 1.05645 |
| Calculation time (sec) | 112 | 139 | - | - |
| # of NLG (or outer) iterations | 11 | 15 | - | - |

Fig. 4, Table V, and Table VI show the transient results. As shown in the results, NLG iteration and p-CMFD acceleration give the same results and agreed well with those of other codes. For this problem, NLG iteration shows faster computing performance than p-CMFD acceleration in transient calculations. However, the difference between the computing times is less than 6 % of the total computing time, so the difference can be said to be negligible.

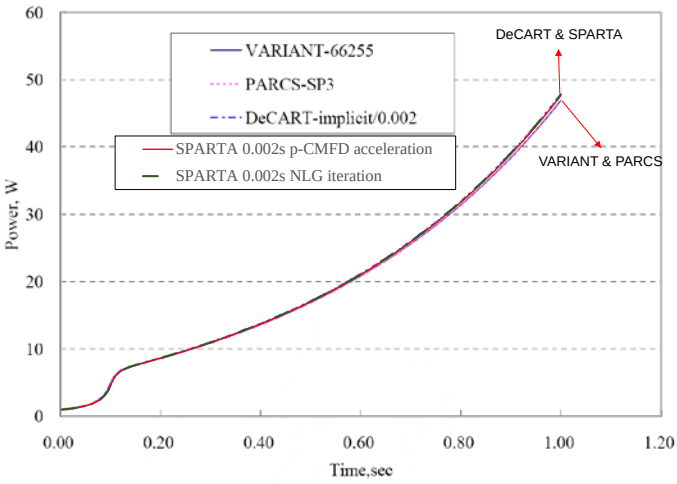


Fig. 4. Power vs time : Mini-core 2D

Table V. Regional power comparison : Mini-Core 2D

| Time | Region | VARIANT-K | DeCART | Error (%) | SPARTA | | | |
|---|---|---|---|---|---|---|---|---|
| | | | | | p-CMFD acceleration | Error (%) | NLG iteration | Error (%) |
| 0.0 | UOXR | 0.562 | 0.562 | -0.05 | 0.562 | -0.07 | 0.562 | -0.07 |
| | UOXF | 1.033 | 1.033 | 0.04 | 1.033 | 0.03 | 1.033 | 0.03 |
| | MOX | 1.076 | 1.076 | 0.01 | 1.076 | -0.03 | 1.076 | -0.03 |
| 0.2 | UOXR | 0.660 | 0.660 | -0.03 | 0.660 | -0.05 | 0.660 | -0.05 |
| | UOXF | 1.031 | 1.031 | 0.04 | 1.031 | 0.03 | 1.031 | 0.03 |
| | MOX | 1.054 | 1.054 | -0.04 | 1.054 | -0.03 | 1.054 | -0.03 |
| 0.4 | UOXR | 0.660 | 0.660 | -0.03 | 0.660 | -0.05 | 0.660 | -0.05 |
| | UOXF | 1.031 | 1.031 | 0.04 | 1.031 | 0.03 | 1.031 | 0.03 |
| | MOX | 1.054 | 1.054 | -0.04 | 1.054 | -0.03 | 1.054 | -0.03 |
| 0.6 | UOXR | 0.660 | 0.660 | -0.03 | 0.660 | -0.05 | 0.660 | -0.05 |
| | UOXF | 1.031 | 1.031 | 0.04 | 1.031 | 0.03 | 1.031 | 0.03 |
| | MOX | 1.054 | 1.054 | -0.04 | 1.054 | -0.03 | 1.054 | -0.03 |
| 0.8 | UOXR | 0.660 | 0.660 | -0.03 | 0.660 | -0.05 | 0.660 | -0.05 |
| | UOXF | 1.032 | 1.031 | 0.05 | 1.031 | 0.04 | 1.031 | 0.04 |
| | MOX | 1.054 | 1.054 | -0.04 | 1.054 | -0.03 | 1.054 | -0.03 |
| 1.0 | UOXR | 0.660 | 0.660 | -0.03 | 0.660 | -0.05 | 0.660 | -0.06 |
| | UOXF | 1.032 | 1.031 | 0.05 | 1.031 | 0.04 | 1.031 | 0.04 |
| | MOX | 1.054 | 1.054 | -0.04 | 1.054 | -0.03 | 1.054 | -0.03 |

Table VI. Computing time for transient : Mini-core 2D

| Code | SPARTA | |
|---|---|---|
| Acceleration | p-CMFD acceleration | NLG iteration |
| Calculation time (hr) | 5.9 | 5.6 |

## 4. Conclusions

NLG iteration with p-CMFD has been successfully extended to have transient capability. As in the steady-state case, NLG iteration and p-CMFD acceleration give identical results if the solutions are converged. In addition, due to the good initial conditions for each time step, the computing performance is very promising in transient calculations compared to p-CMFD acceleration.

Since NLG iteration is natural for parallel computing, the computing performance could be enhanced further if local problems are solved independently with parallel computing nodes. Parallel computing is planned for future work.

## References

[1] M. A. Smith, E. E. Lewis, and B. Na, "Benchmark on deterministic 3D MOX fuel assembly transport calculations without spatial homogenization," *Prog. Nucl. Energy*, **48**, 383 (2006).

[2] S. Yuk, B. Cho, and N. Z. Cho, "Comparison of Non-verlapping Local/Global Iteration Schemes for Whole-Core Deterministic Transport Calculation," *Trans. Kor. Nucl. Soc.*, Gyeongju, Korea, October 24-25 (2013).

[3] N. Z. Cho, "The Partial Current-Based CMFD (p-CMFD) Method Revisited," *Trans. Kor. Nucl. Soc.*, Gyeongju, Korea, October 25-26 (2012).

[4] A. Talamo, "Numerical Solution of the Time-dependent Neutron Transport Equation by the Method of the Characteristics," *J. Comput. Phys.*, **240**, 248 (2013).

[5] J. Y. Cho et al., "Transient Capability of the DeCART Code," KAERI, KAERI/TR-2930 (2005).

[6] L. A. Hageman and J. B. Yasinsky, "Comparison of Alternating-Direction Time-Differencing Methods with Other Implicit Methods for the Solutions of the Neutron Group-Diffusion Equations," *Nucl. Sci. Eng.*, **38**, 8 (1969).

[7] H. G. Joo et al., "Methods and Performance of a Three-Dimensional Whole-Core Transport Code DeCART," PHYSOR 2004, Lagrange Park, USA, April 25-29 (2004).

[8] A. Rineiski et al., "Time-Dependent Neutron Transport with Variational Nodal Methods," Procs. Joint Int. Conf. Mathematical Method for Supercomputing for Nuclear Applications, Saratoga Springs, New York, October (1997).

[9] T. Taiwo et al.,"Development of a Three-Dimensional Transport Kinetics Capability for LWRMOX Analysis," *Trans. Am. Nucl. Soc.*, **79**, 298 (1998).